Supplementary Information (SI) for Journal of Materials Chemistry A.

Fire-safe polymer composites led by nature-inspired MOF-derived single atom catalysis strategy for thermal management with recyclability

Xue Bi[a], Jinhu Hu[a], Zeqi Zhang[a], Ye-Tang Pan[a*], Wenchao Zhang[a], Jun Sun[c, d], Xiaodong Qian[b], Pingan Song[e, f], Jiyu He[a*], Rongjie Yang[a]

[a] *National Engineering Research Center of Flame Retardant Materials, School of Materials Science & Engineering, Beijing Institute of Technology, Beijing 100081, PR China*

[b] *Beijing Key Laboratory of Metro Fire and Passenger Transportation Safety, China Academy of Safety Science and Technology, Beijing, 100012, China*

[c] *State Key Laboratory of Organic-Inorganic Composites, Beijing University of Chemical Technology, 100029, PR China*

[d] *Beijing Key Laboratory of Advanced Functional Polymer Composites, Beijing University of Chemical Technology, Beijing 100029, PR China*

[e] *School of Agriculture and Environmental Science, University of Southern Queensland, Springfield Central, QLD 4300, Australia*

[f] *Centre for Future Materials, University of Southern Queensland, Springfield Central, QLD 4300, Australia*

*Corresponding author: Ye-Tang Pan; Jiyu He.

E-mail address: pyt@bit.edu.cn; hejiyu@bit.edu.cn

Experimental

Characterization

X-ray diffraction (XRD) was employed on an X-ray diffractometer (DX-2600, Rigaku, Tokyo, Japan), using Cu Kα radiation (Kλ=1.5418 Å), at a scanning rate of 0.01 °/s.

Scanning electron microscope (SEM) and Energy dispersive X-ray spectrometry were performed on a Regulus8230 (Hitachi, Japan) at the accelerating voltage of 15 kV. Electron Distribution Spectroscopy (EDS) was performed with X-Max (Oxford).

Transmission electron microscopy (TEM) was employed on a Tecnai G2 F20 S-TWIN (FEI, America) at 300 kV and a tungsten filament transmission electron microscope (JEM 1200EX, JEOL, Japan) operated at 100 kV. The carbon membrane support was supplied by Beijing Zhongjingkeyi Technology Co. Ltd.

X-Ray photoelectron spectroscopy (XPS) spectra was conducted by using an Thermo Scientific K-Alpha X-ray photoelectron spectrometer (Thermo Fisher Scientific).

The nitrogen sorption isotherms of the samples were examined using an ASAP 2460 analyzer (MICROMERITICS INSTRUMENT CORP, USA) employing the BET method.

High-angle annular dark-field scanning transmission electron microscopy (HAADF-STEM) images were obtained at 300 kV with a Thermo Scientific Themis Z.

Raman spectroscopy was studied the structure components of the residual char of PUA composites by a Renishaw in Via confocal microscope Raman system (Renishaw, UK) with a 633 nm laser source.

Thermogravimetric analysis (TGA) was performed by using a thermogravimetric analyzer (Mettler-Toledo, Zurich, Switzerland) with the specimen weight of 8 mg at a heating rate of 10°C/min under nitrogen. The authors extend their gratitude to Mr. Shuai Xingpeng from Shiyanjia Lab (www.shiyanjia.com) for providing invaluable assistance with the TG analysis.

Limiting oxygen index (LOI) was tested by g an oxygen index analyzer (Rheometric Scientific Ltd., Hampshire, UK) with the specimen dimension of 130 ×

6.5 × 3 mm^3 according to ASTM D 2863 procedure.

Cone calorimeter test (cone) was performed to study the fire performance of PUA composites according to the standard of ISO 5660 by a microscale combustion calorimeter (GOVMARKMCC-2) at a heat flux of 50 kW/m^2.

Thermogravimetric analysis-infrared spectrometry (TG-IR) was performed using a STA 8000 thermogravimetric analyzer (Perkin Elmer) interfaced to the Frontier FT-IR spectrophotometer (Perkin Elmer) at a heating rate of 10°C/min under nitrogen. The FT-IR specimen cell was kept at 280°C.

The hardness of all TPU materials was assessed using a Shore hardness tester (HPE II, Bareiss) and averaged over the five points of each sample.

The contact angle of all fillers and TPU materials with water, as well as the contact angle of all fillers with ethylene glycol, was evaluated using a contact angle meter (Germany-Dataphysics-OCA20) and averaged the two points for each sample.

The UV-vis absorption spectra of TPU samples were measured using a UH4100 spectrometer (Hitachi, Japan) in the range of 200-900 nm at room temperature.

The mechanical properties of the splines were tested using an electronic tensile testing machine (DXLL-5000, Shanghai D & G Measure Instrument Co. Ltd., China) operated at a rate of 10 mm/min.

DSC measurements were performed with DSC214 (NETZSCH, Germany) at a heating rate of 10°C/min and a cooling rate of 5°C/min. The specific test process is to raise the temperature to 250°C, then cool down to -100°C, and then increase the temperature to 250°C.

Results and discussions

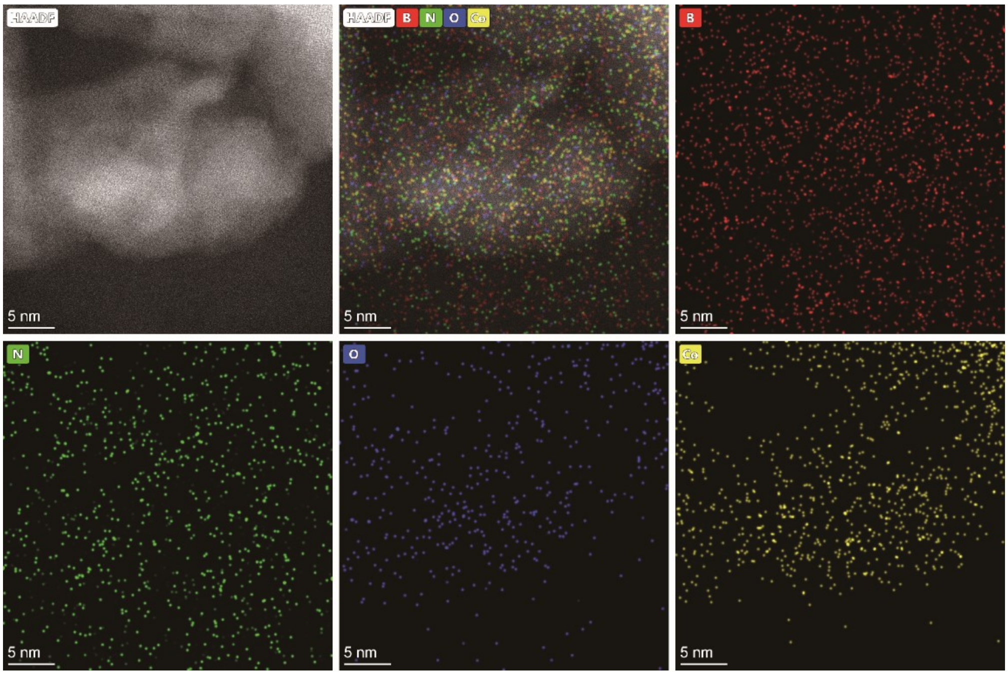

Figure S1. STEM and corresponding TEM mapping images.

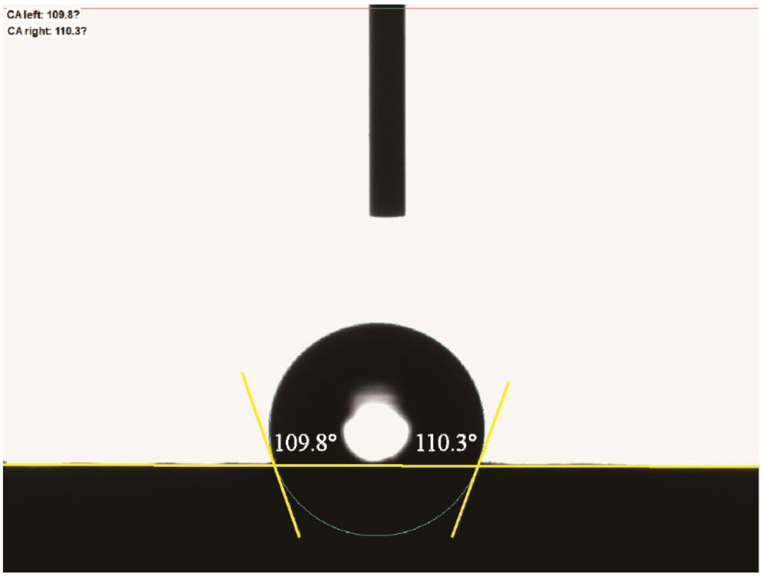

Figure S2. Water contact angles of pure TPU.

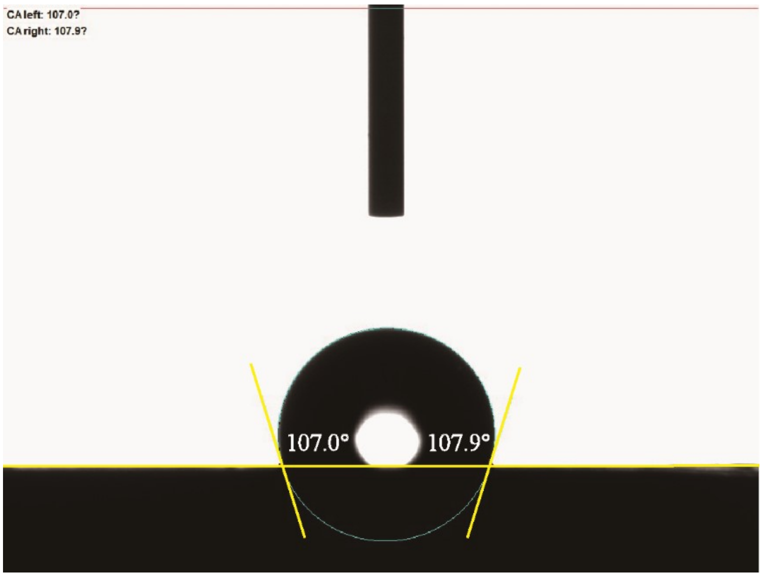

Figure S3. Water contact angles of TPU/ZIF-67.

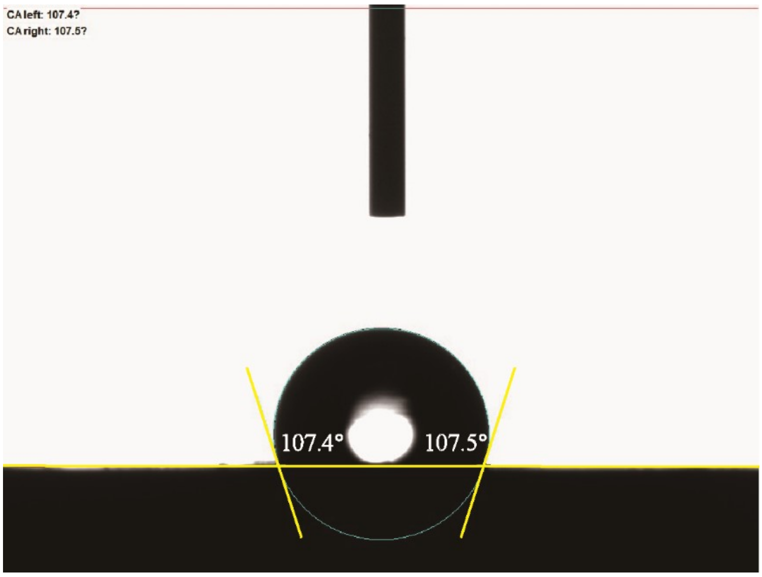

Figure S4. Water contact angles of TPU/NH_2-ZIF-67.

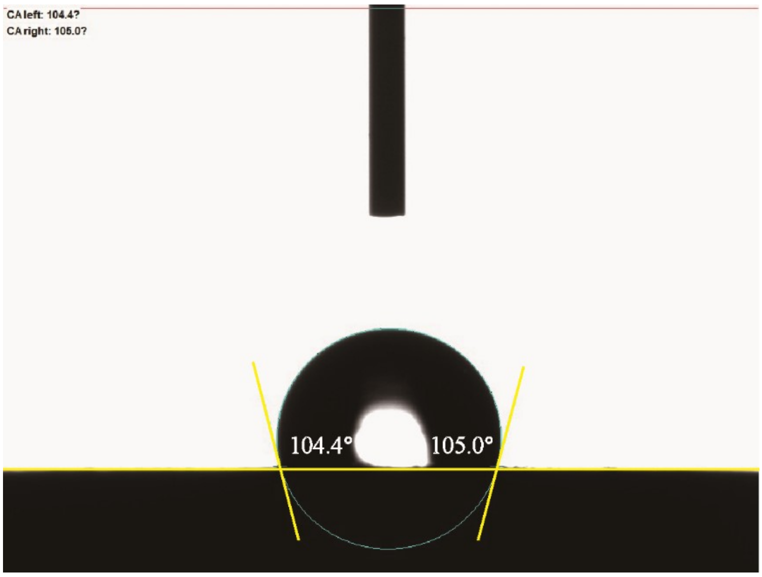

Figure S5. Water contact angles of TPU/BA@NH_2-ZIF-67.

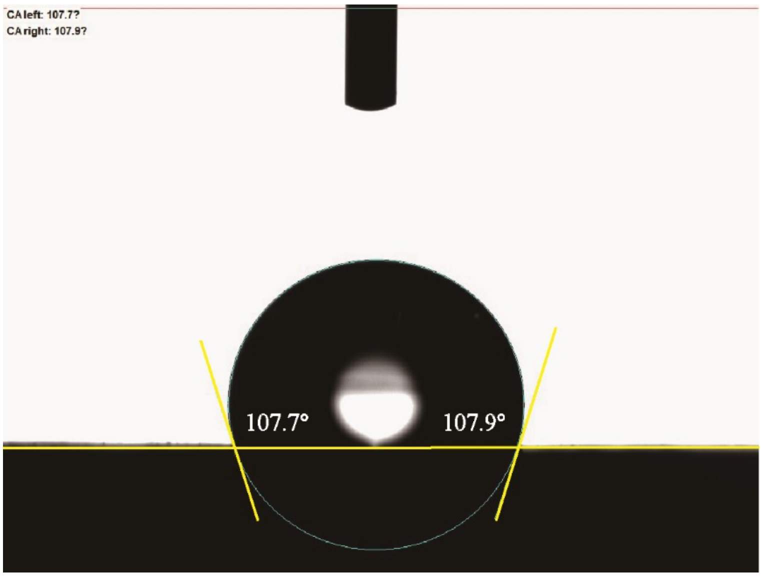

Figure S6. Water contact angles of TPU/h-BNNSs@Co.

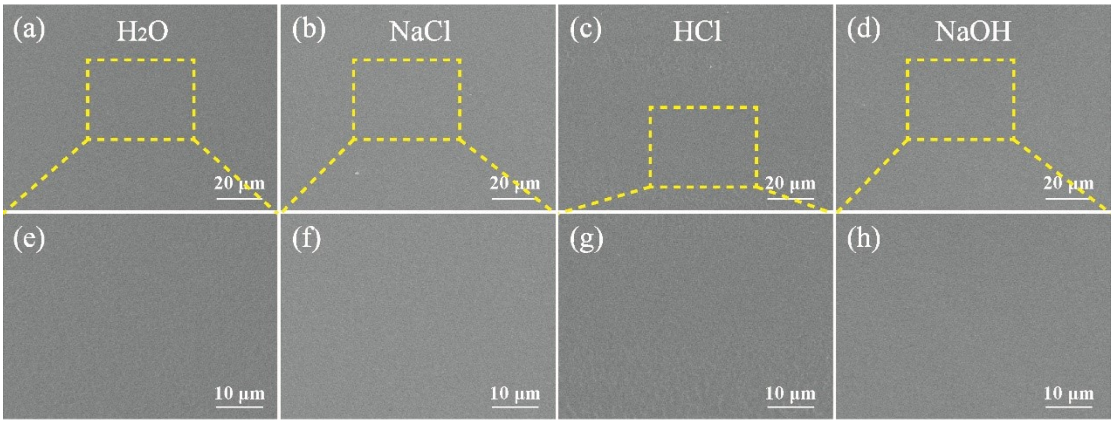

Figure S7. SEM image and enlarged SEM image of the fractured surface of pure TPU after 60 days of the chemical resistance test.

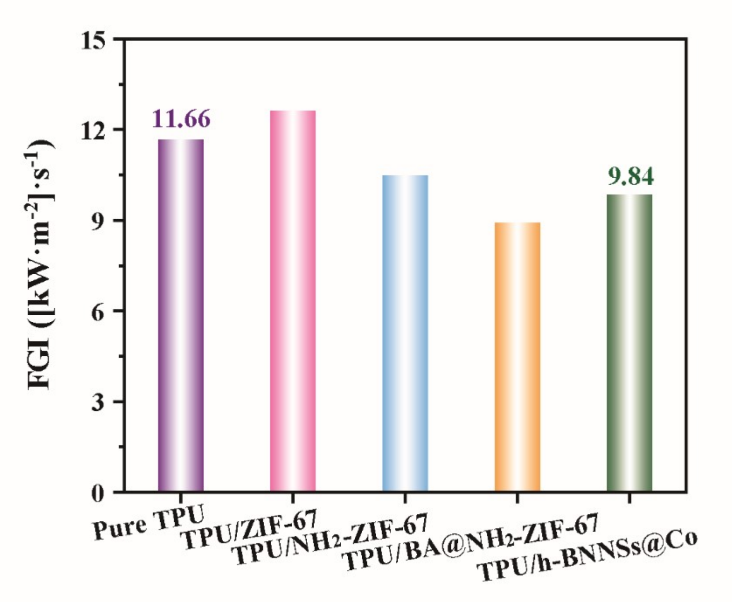

Figure S8. FGI of pure TPU and TPU composites.

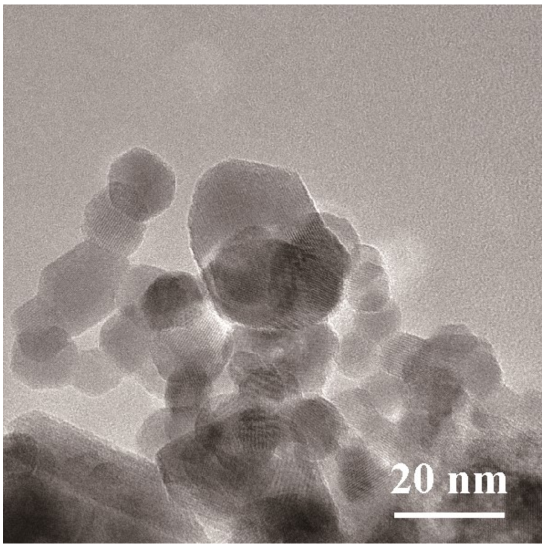

Figure S9. TEM image of the recovered materials.

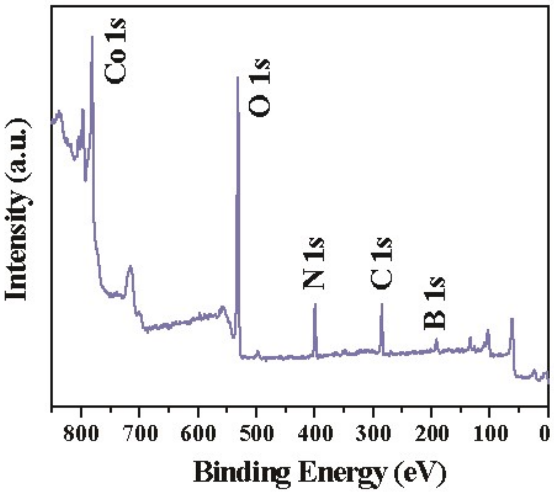

Figure S10. XPS spectra of the recovered materials.

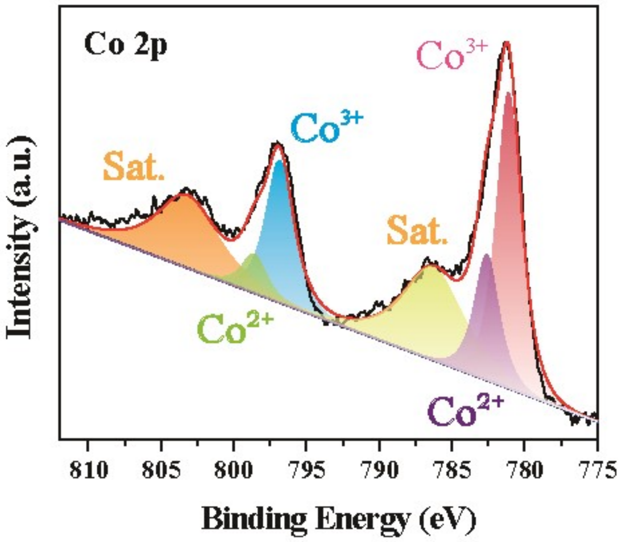

Figure S11. XPS Co 2p spectra of the recovered materials.

Table S1. Thermal decomposition data of hybrid materials in N_2.

Samples	$T_{5\%}$ (°C)	T_{max} (°C)	R_{max} (%/°C)	$Char_{800°C}$ (%)
ZIF-67	548.6	567.7	-0.37	58.2
NH_2-ZIF-67	241.2	489.9	-0.39	46.9
BA@NH_2-ZIF-67	210.6	487.8	-0.32	50.5
h-BNNSs@Co	-	-	-	100.1

Table S2. Tensile strength and Elongation of TPU and TPU composites.

Sample	Tensile strength (MPa)	Elongation at the break (%)
pure TPU	28.58±1.08	432.05±15.26
ZIF-67	19.73±0.67	326.41±9.86
NH_2-ZIF-67	20.89±1.02	328.43±10.24
BA@NH_2-ZIF-67	23.56±0.98	378.07±9.18
h-BNNSs@Co	25.03±1.29	402.23±13.45

Table S3. Contact angle data and surface energy results for TPU and the hybrids.

Sample	Contact angle (degrees)		γ_{SV}^{d} (MJ·m^{-2})	γ_{SV}^{p} (MJ·m^{-2})	γ_{SV} (MJ·m^{-2})	γ_{12} (MJ·m^{-2})
	θ（water）	θ（ethylene glycol）				
pure TPU	110.9±2.6	89.7±1.5	15.21	0.53	15.74	-
ZIF-67	66.1±1.6	36.1±0.7	23.57	15.91	39.48	11.54
NH_2-ZIF-67	72.3±1.2	43.0±0.5	25.09	11.37	36.46	30.21
BA@NH_2-ZIF-67	53.2±1.1	45.2±0.5	4.84	45.06	48.90	38.70
h-BNNSs@Co	77.8±1.9	60.5±0.8	12.68	14.79	27.47	9.84

Table S4. Contact angle data of TPU and TPU composites.

Sample	Contact angle (degrees)
pure TPU	110.1±0.3
TPU/ZIF-67	107.5±0.4
TPU/NH_2-ZIF-67	107.5±0.1
TPU/BA@NH_2-ZIF-67	104.7±0.3
TPU/h-BNNSs@Co	107.8±0.1

Table S5. Shore hardness data of TPU and TPU composites.

Sample	1	2	3	4	5	Average value
pure TPU	90.2	90.5	90.0	90.3	90.5	90.3
TPU/ZIF-67	91.6	91.9	91.3	92.0	91.5	91.7
TPU/NH_2-ZIF-67	91.5	91.6	91.1	91.4	91.4	91.4
TPU/BA@NH_2-ZIF-67	91.0	91.3	91.8	91.1	91.3	91.3
TPU/h-BNNSs@Co	92.3	92.8	92.4	91.9	92.1	92.3

Table S6. Thermal decomposition data of TPU and TPU composites.

Samples	$T_{5\%}$ (°C)	T_{max} (°C)	R_{max} (%/°C)	$Char_{800°C}$ (%)
pure TPU	297.3	404.2	-1.04	11.0
TPU/ZIF-67	249.5	326.2	-0.90	17.3
TPU/NH_2-ZIF-67	281.8	325.5	-1.10	19.1
TPU/BA@NH_2-ZIF-67	281.8	322.8	-0.99	21.7
TPU/h-BNNSs@Co	300.2	404.2	-0.90	23.6

Table S7. Thermal conductivity of pure TPU and TPU composites.

Samples	Thermal conductivity ($W \cdot mK^{-1}$)	TC enhancement (%)
pure TPU	0.29	-
TPU/ZIF-67	0.36	24.5
TPU/NH_2-ZIF-67	0.34	16.6
TPU/BA@NH_2-ZIF-67	0.36	22.8
TPU/h-BNNSs@Co	0.41	42.8

Table S8. Tensile strength and Elongation of TPU and TPU composites after 60 h UV irradiation.

Sample	Tensile strength (MPa)	Elongation at the break (%)	Retention of tensile strength (%)	Retention of elongation at break (%)
pure TPU	14.16±1.02	272.97±8.04	49.55	63.18
TPU/ZIF-67	11.20±0.98	275.40±8.26	62.02	81.93
TPU/NH_2-ZIF-67	14.43±0.95	332.09±9.75	71.97	90.85
TPU/BA@NH_2-ZIF-67	18.72±1.54	301.02±10.24	88.67	86.87
TPU/h-BNNSs@Co	17.47±1.14	376.39±10.18	69.80	93.58

Table S9. Thermal decomposition data of TPU and TPU composites after 60 h UV irradiation.

Samples	$T_{5\%}$ (°C)	T_{max} (°C)	R_{max} (%/°C)	$Char_{800°C}$ (%)
pure TPU	292.1	310.8	-0.83	8.5
TPU/ZIF-67	286.8	322.6	-1.35	10.2
TPU/NH_2-ZIF-67	290.0	328.8	-1.41	12.5
TPU/BA@NH_2-ZIF-67	273.9	331.8	-1.20	10.8
TPU/h-BNNSs@Co	303.1	409.6	-0.73	11.5

Table S10. Weight changes curves of pure TPU in deionized water, 3.5 wt.% NaCl aqueous solution, 3.5 wt.% HCl aqueous solution and 3.5 wt.% NaOH aqueous solution.

Times (day)	H_2O (wt. %)	NaCl (wt. %)	HCl (wt. %)	NaOH (wt. %)

10	1.266	1.318	1.311	1.353
20	1.931	2.031	2.265	2.297
30	2.293	2.405	2.772	2.861
40	2.566	2.637	3.032	3.133
50	2.698	2.812	3.231	3.253
60	2.808	2.926	3.313	3.371

Table S11. Weight changes curves of TPU/h-BNNSs@Co in deionized water, 3.5 wt.% NaCl aqueous solution, 3.5 wt.% HCl aqueous solution and 3.5 wt.% NaOH aqueous solution.

Times (day)	H_2O (wt. %)	NaCl (wt. %)	HCl (wt. %)	NaOH (wt. %)
10	0.729	0.427	0.546	1.985
20	1.204	0.878	0.969	3.264
30	1.755	1.203	1.325	4.039
40	2.128	1.426	1.552	4.721
50	2.359	1.652	1.754	5.227
60	2.586	1.799	1.995	5.545

Table S12. Combustion parameters after cone of TPU and TPU composites.

Samples	pure TPU	TPU/ZIF-67	TPU/NH_2-ZIF-67	TPU/BA@NH_2-ZIF-67	TPU/h-BNNSs@Co

LOI (%)	21.2	23.2	23.0	23.5	25.6
pHRR (kW/m^2)	1124±31	694±15	681±20	624±21	590±12
THR (MJ/m^2)	87±9	85±6	80±7	70±5	56±5
pSPR (m^2/kg)	0.164±0.011	0.060±0.009	0.063±0.008	0.092±0.011	0.091±0.007
TSP (m^2)	14.66±0.6	11.81±0.8	11.05±0.5	13.18±0.5	6.51±0.7
tpSPR (s)	105±10	50±5	40±5	65±5	55±5
pCOP (g/s)	0.0129±0.0010	0.0045±0.0007	0.0051±0.0008	0.0063±0.0008	0.0063±0.0006
pCO$_2$P (g/s)	0.74±0.12	0.41±0.09	0.41±0.08	0.38±0.08	0.35±0.05

Table S13. Comparison of increase in char residue and reduction in pCOP in literature.

Additive amount	Reduction in pCOP (%)	Increase in char residue (%)	Ref.
4%	-30	26.1	[47]
4%	-10.0	22.0	[47]
4%	6.7	21.5	[47]
2%	24.3	10.8	[48]
3 wt.%	30.8	23.3	[49]
2 wt.%	42.9	27.4	[50]
3 wt.%	51.3	24.5	[51]
6.8 wt.%	27.8	52.5	[52]
5.97 wt.%	33.3	63.0	[53]
5 wt.%	51.2	54.4	This work

Table S14. Comparison of heat release, smoke release of TPU/h-BNNSs@Co nanocomposites with other TPU nanocomposites previously reported.

Samples	Contents	pHRR	THR	pSPR	TSP	pCOP	Ref.

		(kW/m^2)	(MJ/m^2)	(m^2/kg)	(m^2)	(g/s)	
TPU-6	3 wt.%	-40.0%	-14.5%	-58.8%	-47.5%	-57.7%	[1]
TPU/CNTs/BMO-1.0	3%	-39.0%	-15.3%	-37.3%	-27.9%	-41.8%	[2]
TPU/Cu0.0625	2 wt.%	-26.0%	-1.3%	-1.0%	/	/	[3]
TPU/MOF@MH-P	2 wt.%	-45.8%	/	-46.7%	-21.4%	-37.4%	[4]
TPU/CTAB-BN-4.0	3%	-57.5%	-17.7%	/	/		[5]
TPU/h-BN@SiO$_2$@PA-2.0	2 wt.%	-23.5%	-22.1%	-29.2%	-8.6%	/	[6]
TPU/h-BNNSs@Co	5 wt.%	-47.5%	-35.6%	-44.5%	-55.6%	-51.2%	This work

Table S15. Thermal decomposition data of TPU composites.

Samples	C-C/C-H area (%)	C-O area (%)	C=O area (%)	Cox/Ca
Pure TPU	55.58	25.54	18.89	79.94
TPU/h-BNNSs@Co	66.02	17.68	16.30	51.47

References

1. C. Shi, M. Wan, Z. Hou, X. Qian, H. Che, Y. Qin, J. Jing, J. Li, F. Ren, B. Yu and N. Hong, *Polym. Degrad. Stab.*, **2022**, 204, 110119.
2. Y. Hou, C. Liao, S. Qiu, Z. Xu, X. Mu, Z. Gui, L. Song, Y. Hu and W. Hu, *Chem. Eng. J.*, **2022**, 428, 132338.
3. X. Chen, X. Chen, S. Li and C. Jiao, *Polym. Adv. Technol.*, **2021**, 32, 2829-2842.
4. B. Tu, K. Zhou, Q. Zhou, K. Gong and D. Hu, *RSC Adv.*, **2021**, 11, 9942-9954.
5. W. Cai, X. Mu, Y. Pan, W. Guo, J. Wang, B. Yuan, X. Feng, Q. Tai and Y. Hu, *Polym. Adv. Technol.*, **2018**, 29, 2545-2552.
6. W. Cai, B. Wang, L. Liu, X. Zhou, F. Chu, J. Zhan, Y. Hu, Y. Kan and X. Wang, *Compos. B. Eng.*, **2019**, 178, 107462.